Canadian Conference - Pacific Conference on Earthquake Engineering 2023

Vancouver, British Columbia

June 25th – June 30th, 2023

Experimental Investigation of Exposed Column Base Plate Connections Subjected to Combined Axial and Bi-Directional Lateral Loading

Kyle Roller[1], AHM Muntasir Billah[2*] Ahmed Elshaer[1], Asif Iqbal[3]

[1] Lakehead University, Department of Civil Engineering, Thunder Bay, ON, Canada, P7A 7T8
[2] University of Calgary, Department of Civil Engineering, Calgary, AB, Canada, T2N 1N4
[3] University of Northern British Columbia, Prince George, BC, Canada, V2N 4Z9
[*] muntasir.billah@ucalgary.ca

ABSTRACT

Column base plate (CBP) connections are critical components in the overall design of a steel structure. CBP connections are responsible for transferring the forces exerted on base columns through a base plate and grout pad into a concrete foundation utilizing anchor rods. Exposed-type column bases are widely used in low-rise building construction all over the world. Current design codes and guidelines do not address adequately the design of these exposed CBP connections under combined axial load and bi-axial bending. Practicing engineers often adopt complex finite element method or design them in two directions separately, which often results in overly conservative design. A more direct approach to designing CBP connections subjected to combined axial and lateral loading conditions would help ensure column base connections perform as intended under extreme loading. The inadequate design of a CBP connection will cause the failure of the connection before the column can reach its peak design values. This configuration is known as a "Strong Column / Weak Connection". This failure is initiated by the inelastic deformation of one or more of the following components: anchor rods, concrete, grout, weld or base plate. The design of all these components will have a combined effect on the CBP connection's stiffness, strength, and deformation capacity. The objective of this research is to perform an experimental study to investigate the behavior of exposed CBP connections subjected to axial and bi-directional lateral loading. Four large-scale CBP connection specimens have been experimentally tested under combined axial and bi-directional lateral loading to observe the effects of varying anchor rod pattern and base plate thickness. The results indicate that the failure mode was governed by strong column/weak connection. Also, base connection with eight bolts showed higher rotational stiffness compared to connection with four bolts.

Keywords: Column-Base Plate Connection; Axial Load, Bi-Axial Bending, Experiment, Cyclic Loading.

INTRODUCTION

Background

Ensuring adequate seismic performance of a structure during a major seismic event is a growing concern across the world. Many buildings utilize exposed column base plate connections designed to resist forces only in the major direction, although the columns are designed for resisting bi-axial bending. Some of these connections may not consider the base plate uplift condition, where lateral forces are not accounted for in the base connection design. To combat this issue the SAC Joint Venture [1] was formed to investigate damage to welded steel moment frame buildings from the 1994 Northridge earthquake. The goal of the SAC Joint Venture was to help develop new design approaches to help steel frame buildings perform more adequately when subjected to earthquakes [1].

Previous studies have been conducted by DeWolf and Sarisley [2] and Drake and Elkin [3] to progress the design of base connections to account for combined axial load and moment. The American Institute of Steel Construction's Steel Design Guide-1 by Fisher and Kloiber [4] provides a detailed design guideline for base connections commonly used for current base connection design to meet combined axial load and moment demands. Gomez [5] further investigated the design guide-1 approach and extensively reviewed base connection design to meet cyclic loading only in the major direction.

Currently, there is minimal research pertaining to the design of exposed column base connections subjected to a combined axial load and bi-directional lateral loading. The difficulty lies in designing the base connection to act as a fixed connection in both the strong and weak axes. Buildings can become mechanically unstable when base plate connections are combined with pinned beam-column connections [6]. This can be resolved by utilizing a fixed column base or a rigid beam-column connection to achieve stability. Both approaches can be costly and overly conservative for low to mid-rise buildings composed of low-mass sections. Choi and Choi [7] conducted an experimental investigation on the inelastic behavior for exposed-type steel HSS column bases under three-dimensional loadings. They concluded that the failure patterns of exposed-type column bases are significantly different under combined axial and bi-axial bending compared to uniaxial bending. However, they did not provide any design equations or guidelines that can be used for design of such base plates. Recently, Fasaee et al. [8] conducted a numerical investigation to evaluate the capacity of flexible column-base connections under axial load and bi-axial bending. Seco et al. [9] investigated the response of exposed column base-plates with four outer anchor bolts subjected to monotonic bi-axial bending. They concluded that the rotational stiffness and bending resistance of base-connections are dependent on the direction of the applied moment. Cloete and Roth [10] proposed a simplified theoretical model for designing column base connections subjected to axial load and bi-axial bending. However, the proposed method is conservative and does not consider the effect of loading cycles. However, there exists no study that experimentally investigated the performance of column-base connections under combined axial load and biaxial cyclic bending moment. This study aims to experimentally investigate the behavior of exposed column-base connections subjected to combined axial load and bi-axial moment. Key responses obtained from the experiments include base connection moment-rotation response, anchor rod forces, base plate deformation, and failure modes. Although four specimens are tested, results from two specimens, one with four bolts and another with eight bolts, are presented herein. It was found that the 8-bolt configuration has a greater moment capacity in both the major and minor directions when compared to the 4-bolt one.

Base Connection Failure Categories

Fahmy [11] presented a thorough formulation for base connection design which directly relates to three main categories of failure. The first category is Strong Column / Weak Connection failure which is initiated by the inelastic deformation of one or more of the following components: anchor rods, concrete, grout, weld, and base plate. There are six modes of failure associated with a Strong Column / Weak Connection. The first four failure modes are typically caused by an undersized base plate and are classified by the formation of yield lines along the column flanges and in between the anchor rod holes of the baseplate. The fifth mode is related to the yielding of the anchor rods (shown in Figure 1a). This occurs mainly when the anchor rods are undersized and the base plate is oversized. This mode exhibits a pinched hysteresis response caused by cumulative elongation of the anchor rod. The strength of the connection will also drop quickly during repeat cycles at the same drift level. The sixth mode is caused by simultaneous yielding of both anchor rods and base plate. This occurs mainly when both the base plate and the anchor rod are undersized.

The second category of failure is a Weak Column / Strong Connection which is displayed in Figure 1b. This failure mode is defined by a plastic hinge forming in the column only. Connections which fail in this mode have high ductility with stable hysteresis loops, and increased strength after yielding. This failure mode allows the column to reach its peak design values before failure. This failure category can be identified when buckling occurs in the column flanges before any other components begin to yield as shown in Figure 1b. The final category is balanced failure where yielding of the base connection and column occurs simultaneously as shown in Figure 1c.

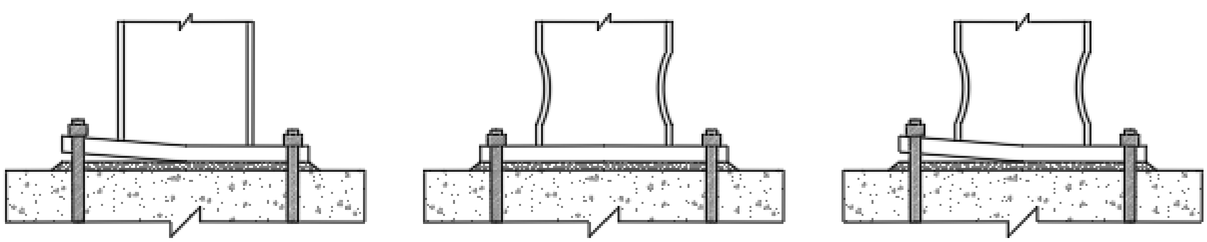

(a) (b) (c)

Figure 1. Exposed Column Base Connection Failure Categories: (a) Strong Column / Weak Connection, (b) Weak Column / Strong Connection, (c) Balanced.

EXPERIMENTAL PROGRAM

Test Matrix and Description

The test matrix shown in Table 1 displays the differences between the four experiments conducted as a part of this study. Tests 1 and 2 use 4-bolt anchor rod patterns, whereas Tests 3 and 4 use 8-bolt patterns. Tests 1 and 3 use 25mm thick baseplates whereas Tests 2 and 4 use 38mm thick baseplates. The grout height was changed to account for the change in baseplate thickness; this was required so the actuator connection would align properly for all experiments. The baseplate hole patterns for Test 1 and 2 (4-Bolt) and Test 3 and 4 (8-Bolt) are displayed in Figure 2. However, in this paper, the results from Tests 2 and 4 are presented only as the results from other two tests are still in process while this paper is being prepared.

Table 1. Experimental Test Matrix.

Test #	BP Dimensions (mm)	Bolt Pattern	Axial Load (kN)	Lateral Loading	Grout Height (mm)
2	407x407x38	4	400	Bi-Directional	51
4	407x407x38	8	400	Bi-Directional	51

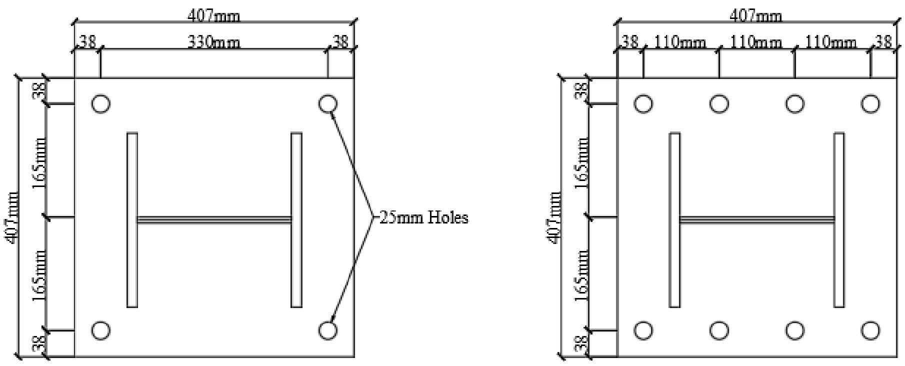

(a) *(b)*

Figure 2. Base Plate Configuration: (a) 4-Bolt Configuration (Test 2), (b) 8-Bolt Configuration (Test 4).

The column section is considered as W250x73 which reflects the typical members that are used as first-story interior columns of steel moment frames in low to high-rise steel buildings in high seismic regions [12]. The length of the column is considered as 1500 mm from the top of the base plate that represents a half-scale column. 12mm fillet welds are used to attach the perimeter of the column base to the baseplate. The cross-sectional dimension of the grout is considered the same as the base plate dimension (407mm x 407mm). A 1520x1520x460 mm concrete footing is considered for the foundation of the column base connection. All columns are produced to meet ASTM A992 standards while the base plates are produced to meet CSA G40.21 (300W) standard. Table 2 depicts the material properties of the components used in the experiments.

Table 2. Material Properties.

Component	Modulus of Elasticity (GPa)	Yield Strength (MPa)	Ultimate Strength (MPa)
W250x73 Column	200	390	524
Base Plate (38mm)	200	363	533
Anchor Rod	200	364	427
Concrete	-	-	32*
Grout	-	-	75*

* denotes the Compressive Strength (f_c') for Concrete and Grout

Test Preparation

The initial process began with constructing the concrete pedestal forms and preparing the rebar cages for each test. 15M bars were used for all the longitudinal bars and stirrup cages. 25M bars were used for the center cage U-bar reinforcement, and hoops. Uniaxial strain gauges were attached to all anchor rods and all wires were run through conduit to the exterior of the footing. Resistances in the gauges were checked before and after the concrete pour. The rods were embedded 400mm (16 inches) inside the concrete pedestal. The bottom (embedded) ends of the anchor rods were attached to 20mm USS washers sandwiched between two grade A hex nuts, which provided the rods with additional strength to resist pull-out. Non-shrink high strength grout was utilized between the column and baseplate and given a minimum of 28 days to cure before testing (similar to concrete). Two pedestals were poured at a time in order to re-use the form. Pedestals were constructed with appropriate lifting hooks so that they could be moved from casting yard to the strong floor. Concrete cylinders and grout cubes were cast to measure the compressive strength of the pedestal concrete and high strength grout on the test day. The concrete and grout strengths are reported in Table 2.

Test Setup

After all concrete pedestals were prepared, the actuators were setup for the experimental testing. The setup required a 250 kN actuator in the N-S direction to apply minor axis bending, a 500 kN actuator in the E-W direction for the major axis bending, and a 500 kN actuator for applying the vertical axial load. Figure 3a shows the setup used for all the tests in the Wood Innovation Research Laboratory at the University of Northern British Columbia. Four tall columns were set into place after the lateral actuators were bolted to the walls. These columns carry the bridge, which bears a 38mm plate connection to the 500 kN vertical actuator. This vertical actuator provides the axial load for all the specimens. The concrete pedestals were fastened to the lab strong floor at four points at 1220mm (4’) on center with 28mm dia. rods and 150mm square plates (12mm thick) to prevent the footing from slippage or uplift. Grade A hex nuts, USS 20mm washers, and 75mm square plate washers (6mm thick) were used to secure the 20mm SAE J429 Grade 2 anchors rods to the base plate. After all final adjustments were made with actuators, the hex nuts were tightened to snug tight plus a ¼ turn.

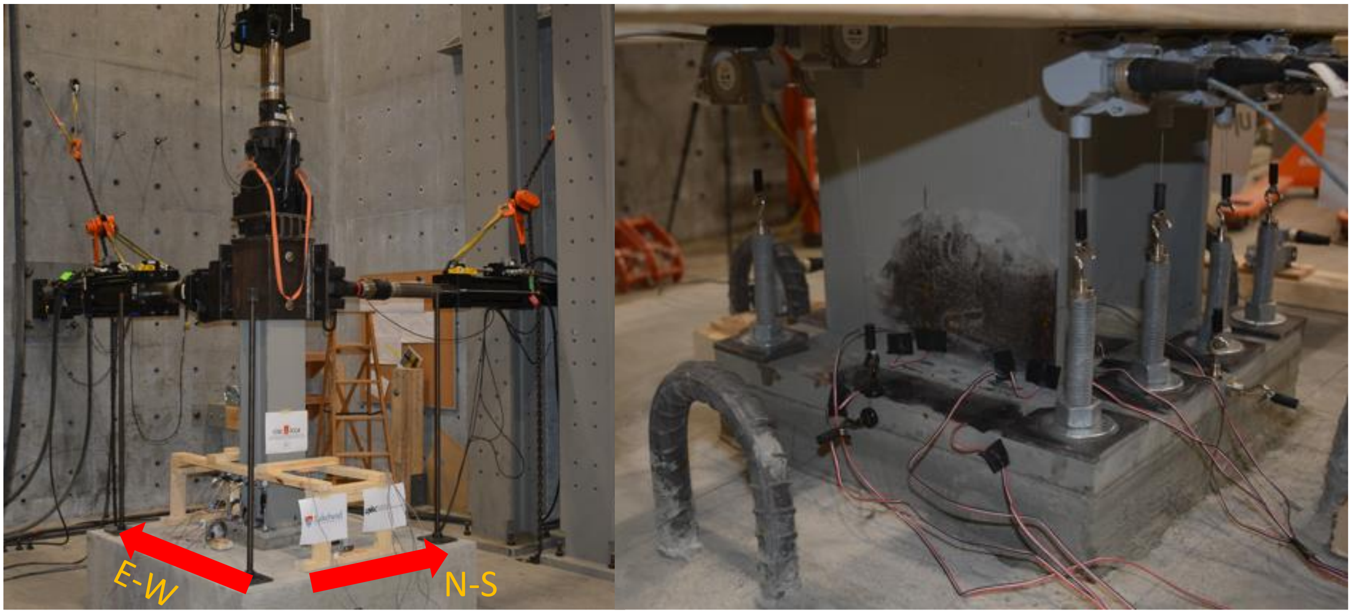

(a) *(b)*

Figure 3. Test Setup: (a) Actuator arrangement, (b) Instrumentation (Test 4 shown).

Actuator Connection

A special connection system was designed to apply load on the steel columns using three actuators simultaneously. Figure 4 shows the details of the connection. The connection was made strong enough to make sure that there was no local buckling in the plates when loads were applied from all three directions as well as to adequately distribute the forces from the major and minor direction actuators through the flange and web of the column, respectively. The connection was made ‘fit to bear’ and was slid into the column from the top and the vertical loading plate firmly sat on the column top. The connection was built-up using 19mm plates. It was made sure there the connection does not move during the tests.

Instrumentation

A total of 30 sensors were used for Test 2 (14 string potentiometers and 16 strain gauges), while 40 sensors (16 string potentiometers and 24 strain gauges) were used for Test 4. String potentiometers were setup to capture the uplifts and lateral slips of the base plate for both E-W (Major) and N-S (Minor) directions. The elongations of all anchor rods were captured using string potentiometers. The forces and lateral displacements produced from the actuators were recorded directly through the actuators using the MTS software. Figure 3b shows the instrumentation setup for the 8-bolt Test (Test-4). Strain gauges were attached to 4 positions on the column and baseplate to capture vertical and horizontal strain respectively and to compare mid-points to edges. Two uniaxial strain gauges were attached to every anchor rod approximately 60mm below the surface of the concrete. All instruments were connected to a Vishay 8000 DAQ system and synchronized data was recorded using strain smart software.

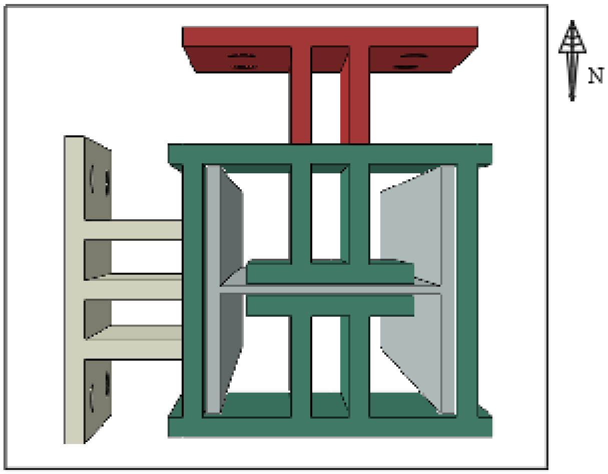

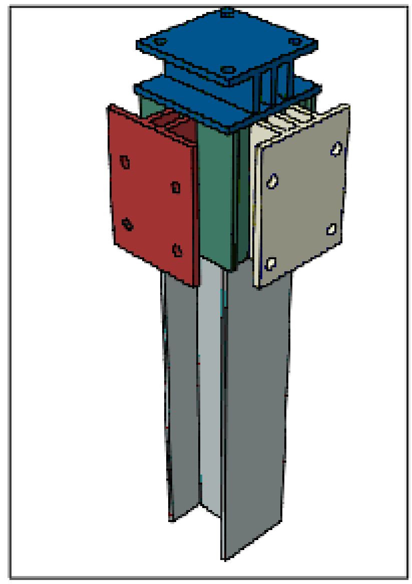

a) *(b)*

Figure 4. Actuator Connection: (a) Plan View, (b) Connection plate connected to column.

Loading Protocol

An elliptical bi-directional lateral loading protocol (Figure 5b) was developed for the experiments. The elliptical protocol was derived from the SAC cyclic loading protocol [1] shown in Figure 5a. The SAC cyclic loading protocol was used in the experimental study by Gomez [5] and a modified version was used in the study by Fahmy [11]. The shape of the elliptical protocol is based on the major lateral drift being twice the size as the minor lateral drift for each cycle. For instance, during the 1.5% major lateral drift cycle the minor drift would reach a max of 0.75% minor lateral drift. Major refers to the E-W direction where the 500 kN actuator attaches to the flange of the column. Minor refers to the N-S direction, where the 250 kN actuator connects to the web of the column (Figure 3a). Similar loading protocol was used of all tests conducted in this study.

The major axis displacement displayed in Figure 5c follows the specified lateral drift cycles of a SAC cyclic loading protocol shown previously in Figure 5a. Some modifications were made to account for transitioning to new cycles which were needed to maintain a bi-directional lateral loading the hydraulic actuators could follow. The cycles were adapted to run within a 1.5 hour time frame. The early major drift cycles which were under 1%, were shortened to run quicker in the beginning of the tests. The cycles after 1% were stretched to account for a quasi-static loading condition.

The minor axis displacement displayed in Figure 5d was developed to form an elliptical motion when applied simultaneously with the major axis displacement. The axial force actuator was programmed to ramp a force of 400 kN over the first 5 minutes (300 sec) of each test. Once the 400 kN is reached the vertical actuator is programmed to keep a constant 400 kN axial load on the specimen until the end of testing. It was decided to stop the tests after 5.5% major lateral drift. Major lateral displacement maxed out at 70mm (E-W direction). Minor lateral displacement maxed out at 35mm (N-S direction).

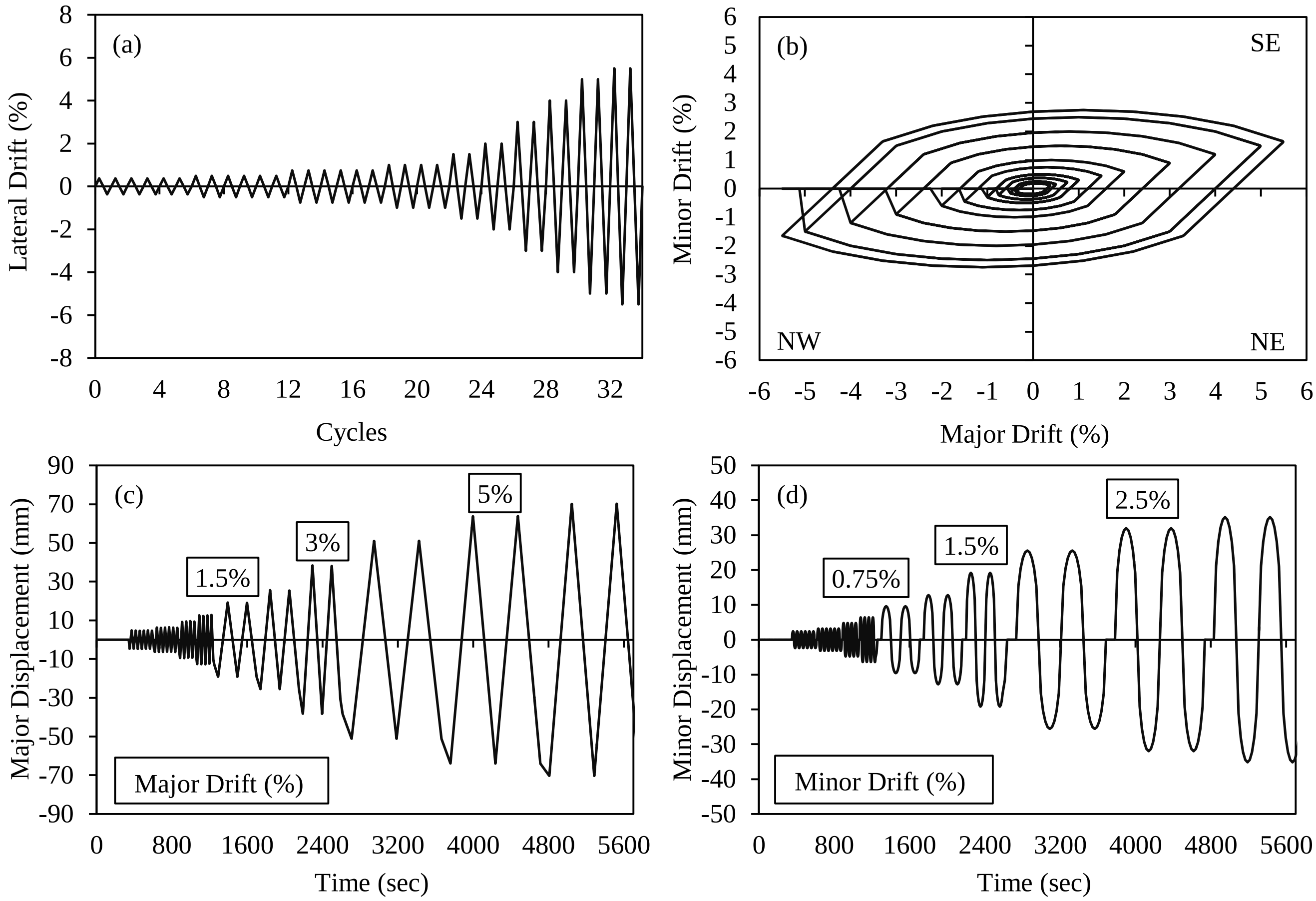

Figure 5. Loading Protocol: (a) SAC Cyclic Lateral Loading Protocol, (b) Bi-Directional Elliptical Lateral Loading Protocol, (c) Major Displacement vs. Time, (d) Minor Displacement vs. Time.

TEST RESULTS

Test results are discussed in the following sections for the two specimens in terms of the column base moment and rotation hysteretic response and base-plate uplift in relation to column drift (%). In addition, the envelope curves from the moment-rotation hysteresis are also obtained. The moment-rotation hysteretic responses were obtained from the experiment under combined axial load and bi-axial bending for both major and minor axes separately. The column base moment (M) and base rotation (θ) are computed from the column lateral force and lateral displacement according to Eq. (1) and Eq. (2), respectively.

$$\boldsymbol{M = F \times H_{col}} \tag{1}$$

$$\boldsymbol{\theta = \left(\Delta_{top} - \left(V \times H_{col}^{3}\right)/(3 \times E_{col} \times I_{col})\right) \times 1/H_{col}} \tag{2}$$

where F is the lateral force at the column top, H_{col} is the column height from the base plate, Δ_{top} is the displacement at the top of the column, E_{col} is the modulus of elasticity of the column, I_{col} is the column's second moment of inertia in the direction of loading.

Test 2 (4-Bolt configuration)

Figures 6a-b show the moment-rotation hysteresis response obtained from test-2 in major and minor directions, respectively. Examination of the hysteretic loops shows that the column base behavior was Strong Column / Weak Connection. The base connection did not show significant ductility. The major axis maximum moment of 116kN.m was reached at 1.2% rotation and then started to decline. The major axis moment capacity dropped by 20% around 2% rotation. Similar behavior was observed in both push and pull directions. While along the minor axis, maximum moment of 55kN.m was reached at 1% rotation and remained stable up to 2% rotation and then started to decline. Figure 6c-d depict the moment-rotation envelope obtained from the hysteresis curve. Figure 6c shows the damage sequence observed in the major axis direction. The base plate uplift was engaged around 1.5% rotation in both push and pull directions. The anchor rods started to yield around 3% rotation. However, no uplift or anchor rod yielding was observed in the minor direction. The results show that the test experienced failure due to anchor rod yielding which categorizes the failure as a Weak Connection / Strong Column. Figure 7a displays the SE anchor rod during the 3% major lateral drift, where Figure 7b shows the test during the final cycle at 5.5% major lateral drift.

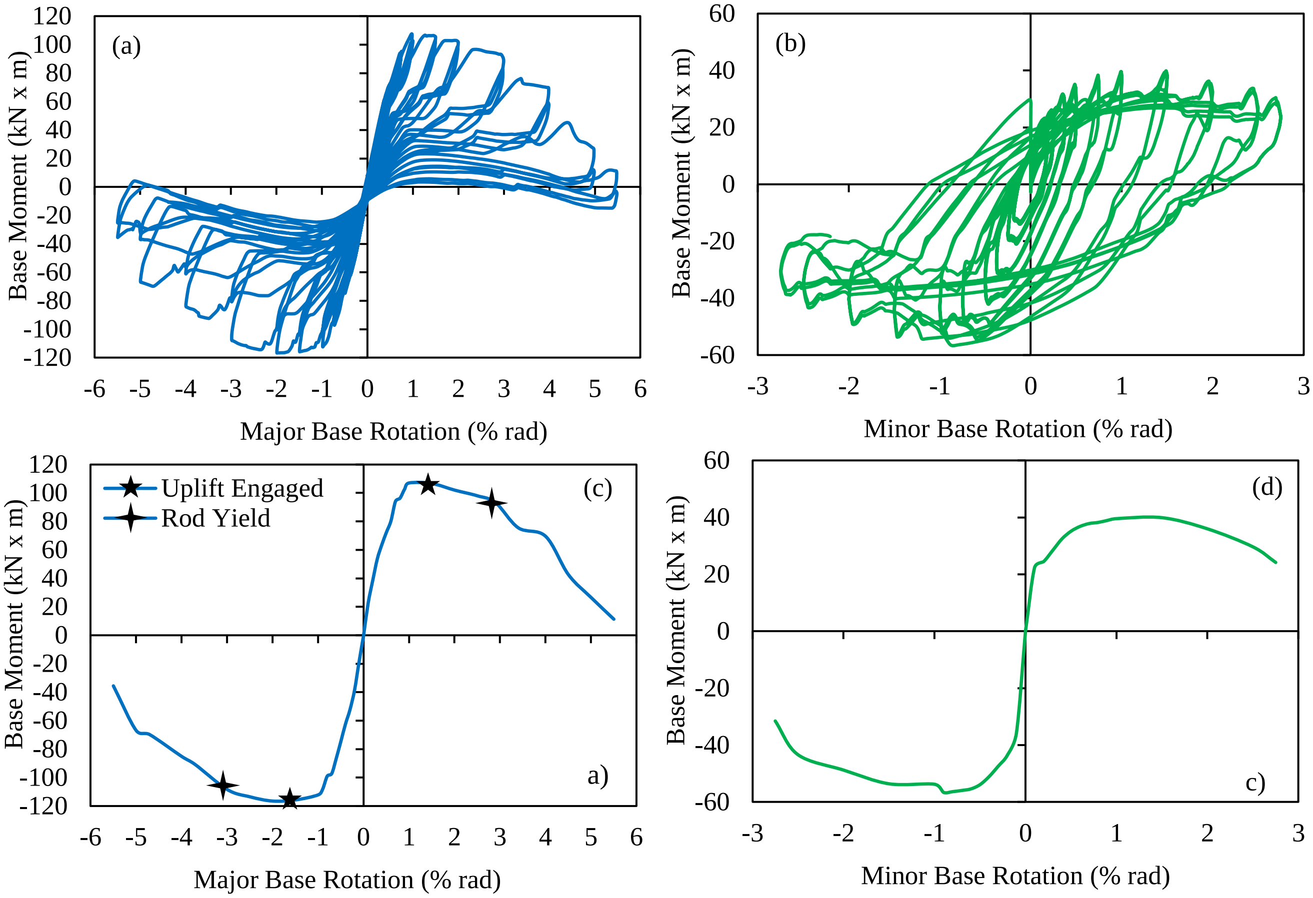

Figure 6. Test 2 Results: (a) Major axis Moment- Rotation (b) Minor axis Moment- Rotation (c) Major axis Moment vs. Base Plate Uplift (East) (d) Minor axis Moment vs. Base Plate Uplift (South)

(a) *(b)*

Figure 7. Test 2 Results: (a) Test 2 - 3% Drift (Rod Yield-red circled) (b) Test 2 - 5.5% Drift (Last Cycle)

Test 4 (8-Bolt Configuration)

Figure 8 shows the moment rotation hysteresis and the envelope curve for the 8-bolt configuration. This specimen also showed similar behavior as 4-bolt configuration. The 8-bolt configuration did not improve the ductility of the base connection. The major axis maximum moment of 121kN.m was reached at 1.7% rotation and then started to decline. The major axis moment capacity dropped by 20% around 3% rotation. Symmetric response was observed in both push and pull directions. The minor axis response was comparable to 4-bolt configuration both in terms of moment and rotation. The hysteric response shows how Test 4 has a fatter hysteresis curve where more energy is dissipated during each cycle due to the additional strength provided by the additional anchor rods. It is also evident that the two tests have very similar responses even though Test 4 has double the number of rods. This is due to the configuration of the rods, where the additional rods are located parallel to the major loading axis. The points at which base plate uplift and anchor rod yielding occurred are labeled in Figure 8c for Test 4. It is found that the base plate uplift was engaged at 1.5 % rad both the East (Push) and West (Pull) directions. For Test 4, the inner rods yield during the 2% major drift cycle (2% rad) after the outer rods yield at 1.5% rad. It was observed that the NW inner rod remained elastic up to 2% rotation and yielding took place at 2% rotation. The NE outer rod also experienced yielding during the 2% major lateral drift cycle at a peak force of 102.6 kN. Test 4 with 8-bolt configuration is also categorized as a Weak Connection / Strong Column due to rod yielding. Figures 9a and b display the base connection during the 2% and 5.5% major lateral drift cycles respectively.

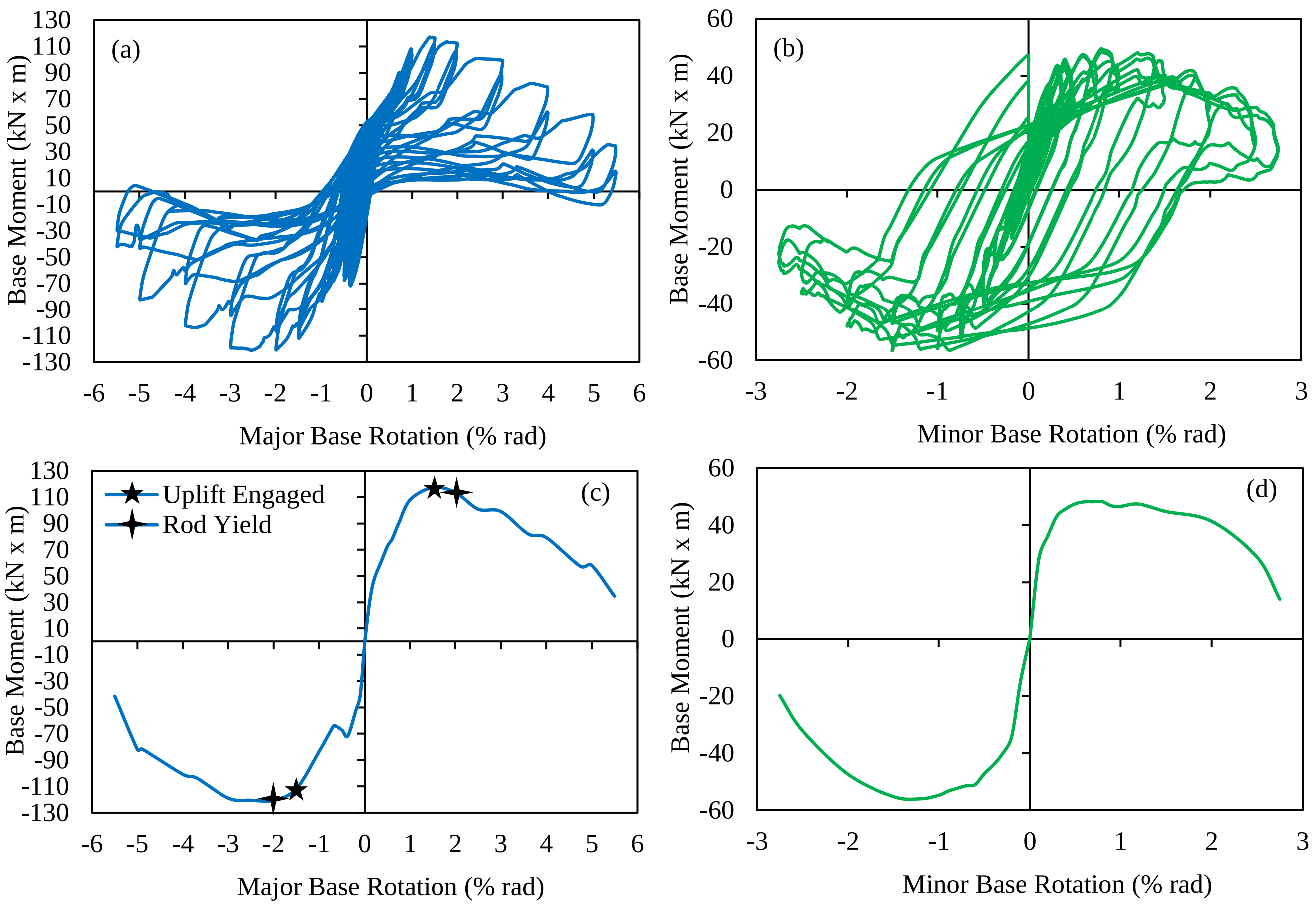

Figure 8. Test 4 Results: (a) Major Base Moment vs. Base Rotation (b) Minor Base Moment vs. Base Rotation (c) Major Base Moment vs. Base Plate Uplift (East) (d) Minor Base Moment vs. Base Plate Uplift (South)

(a) *(b)*

Figure 9. Test 4 Results: (a) Test 4 - 2% Drift (NW Inner Rod Yield-red circle) (b) Test 4 - 5.5% Drift

Resistance to Base Plate Uplift

The maximum base plate uplift (E-W) envelopes for Tests 2 and 4 are displayed in Figure 10a in relation to the major lateral drift cycle. It is shown that Test 2 experiences a maximum major uplift of 16.1mm at the end of the test, whereas Test 4 experiences only 13.9mm uplift. Figure 10b depicts the maximum base plate uplift (N-S) envelopes for Tests 2 and 4 with respect to the minor lateral drift cycle. It is shown that Test 2 experiences a maximum minor uplift of 8.5mm at the end of the test, whereas Test 4 experiences only 6.3mm uplift. The 8-bolt pattern has better resistance to base plate uplift than the 4-bolt pattern while maintaining a greater base moment capacity for both major and minor directions.

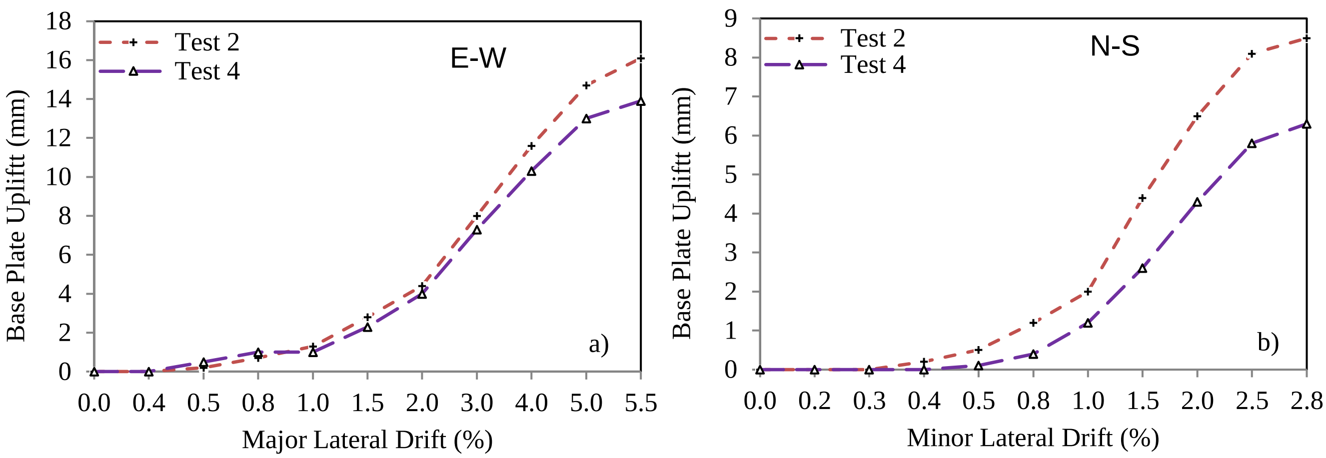

Figure 10. Test Uplift Envelopes Results: (a) Max BP Uplift (E-W) vs. Major Lateral Drift (b) Max BP Uplift (N-S) vs. Minor Lateral Drift

Summary of Test Results

The summary of the experimental test measurements is presented in Table 3. The measurements are the maximum moments of the base connections in the major and minor axis directions, M_{max}; rotational stiffness of the base connection, K_{θ}; the permanent anchor rod elongation at zero displacement at the end of the test, $\Delta_{P\text{-}rod}$; and the maximum tension force in the anchor rods, T_{rod}. Results from Table 3 indicate that, in terms of maximum moment, both specimens showed similar responses. However, due to the presence of four additional bolts, test 4 showed higher rotational stiffness in the major axis direction compared to test 2. The maximum tension force in the anchor rods for both specimens was very similar. However, the anchor rods in test 2 experienced higher permanent anchor rod elongation compared to test 4.

Column-base connection is typically considered as either rigid or pinned during design consideration [13]. Eurocode 3 [14] classifies base connection rigidity into three classes such as rigid, semi-rigid, and pinned depending on the different base rotational stiffness (K_{θ}) limit expressed by Eq. (3), (4) and (5), respectively. Dividing the base moment (M) by the base rotation (θ) the base rotational stiffness can be calculated. Column base connections having base rotational stiffness of

30(EI/H) or greater are considered as fully rigid whereas it is considered as fully pinned when the base rotational stiffness is less than *0.5(EI/H)*. Base connections with rotational stiffness between these two limits are considered to be semi-rigid. According to the rotational stiffness value shown in Table 3, both connections can be classified as fully pinned since the base rotational stiffness is less than *0.5(EI/H)*.

$$K_\theta \geq 30\,(\frac{EI}{H})_{col} \tag{3}$$

$$0.5(\frac{EI}{H})_{col} < K_\theta < 30(\frac{EI}{H})_{col} \tag{4}$$

$$K_\theta < 0.5(\frac{EI}{H})_{col} \tag{5}$$

Table 3. Summary of Test Results

Test No	Direction	M_{max}, kN	K_θ, kN.m/rad	T_{rod}, kN	$\Delta_{p\text{-}rod}$, mm
2	X (major)	116.7	5835	110	14.3
	Y (minor)	56.7	3780		
4	X (major)	121	7118	115	10
	Y (minor)	56	3733		

CONCLUSIONS

This paper presented experimental results of two large-scale column base connections tested under combined axial compression and bi-axial bending. Based on the experimental results, the following conclusions are drawn:

- Both specimens (4 and 8-bolt configuration) are categorized as Weak Connection / Strong Column failures where the connection fails before the column can reach its peak design values.
- The 8-bolt configuration can resist base plate uplift more effectively than the 4-bolt configuration. The 8-bolt configuration has a greater moment capacity in both the major and minor directions when compared to the 4-bolt one.
- Both specimens (4 and 8-bolt configuration) anchor rod yielding as the primary failure mode due to the under sizing of the anchor rods.
- Based on the rotational stiffness values, the connections tested in this study can be classified as a pinned connection.

The results obtained from the experimental study are being used to develop detailed finite element models which will be validated against the experimental results. The finite element models will consider both uni- and bi-axial bending to compare the failure modes and rotational stiffness of column base connections. Detailed parametric study and reliability analysis are underway to propose column-base connection design equations under combined axial compression and bi-axial bending.

ACKNOWLEDGMENTS

This study is based on research supported by the Canadian Institute of Steel Construction (Award no. CISC 2019-04). The financial support is gratefully acknowledged. Any opinions, findings, and conclusions or recommendations expressed in this paper are those of the authors and do not necessarily reflect the views of sponsors. The authors also acknowledge the support provided by the laboratory personnel at Lakehead University and the Wood Innovation Research Laboratory at the University of Northern British Columbia.

REFERENCES

[1] SAC Joint Venture (1994). “SAC Steel Project”. from https://www.sacsteel.org/.

[2] DeWolf J.T., Sarisley E.F. (1980). “Column base plates with axial loads and moments”. *Journal of Structural Division, ASCE*. 106(11), 2167–84.

[3] Drake R.M., & Elkin S.J. (1999). “Beam-column base plate design - LRFD method” *AISC Engineering Journal*, . 36(1), 29–38.

[4] Fisher J.M., & Kloiber L.A. (2006). *Base plate and anchor rod design*. *AISC steel design guide one.* 2nd ed. Chicago, IL: American Institute of Steel Construction.

[5] Gomez, I., Deierlein, G., & Kanvinde, A. (2010). *Exposed Column Base Connections Subjected to Axial Compression and Flexure*. Final Report Presented to the American Institute of Steel Construction (AISC), Chicago, USA.

[6] Lim, W.Y., Lee, D.. & You, Y.C. (2017). "Cyclic loading tests on exposed column-base plate weak-axis connections of small-size steel structures." *Engineering Structures*, 153, 653-664.

[7] Choi, J. H., & Choi, Y. (2013). "An experimental study on inelastic behavior for exposed-type steel column bases under three-dimensional loadings." *Journal of Mechanical Science and Technology*, 27(3), 747-759.

[8] Fasaee, M.A.K., Banan, M.R., & Ghazizadeh, S. (2018). "Capacity of Exposed Column Base Connections Subjected to Uniaxial and Biaxial Bending Moments." *Journal of Constructional Steel Research*, 148, 368–370.

[9] Seco, L., Couchaux, M., Hjiaj, M. & Neves, L.C. (2021). "Column base-plates under biaxial bending moment." *Engineering Structures*, 231:111386.

[10] Cloete, R. & Roth, C.P. (2021). "Column base connections under compression and biaxial moments: Proposed design approach." *Journal of Constructional Steel Research*, 184, 106814.

[11] Fahmy, M. (1999). *Seismic Behavior of Moment-resisting Steel Column Bases*. Ph.D. Dissertation, Department of Civil and Environmental Engineering, University of Michigan, Ann Arbor, Michigan.

[12] Elkady, A., & Lignos, D. G. (2014). "Modeling of the composite action in fully restrained beam-to-column connections: Implications in the seismic design and collapse capacity of steel special moment frames." *Journal of Earthquake Engineering Structural Dynamics*, 43(13), 1935–1954.

[13] Borzouie, J. (2016). *Low Damage Steel Base Connections*. PhD Thesis, Department of Civil and Natural Resources Engineering, University of Canterbury, Christchurch, New Zealand.

[14] Eurocode 3. (2005). *EN 1993-1-8; Design of steel structures – Part 1– 8: Design of Joints*. CEN, European Committee for Standardization, Brussels, Belgium.